

UC San Diego

UC San Diego Previously Published Works

Title

Altered Penile Caveolin Expression in Diabetes: Potential Role in Erectile Dysfunction.

Permalink

<https://escholarship.org/uc/item/2m3743vc>

Journal

The journal of sexual medicine, 14(10)

ISSN

1743-6095

Authors

Parikh, Jay
Zemljic-Harpf, Alice
Fu, Johnny
et al.

Publication Date

2017-10-01

DOI

10.1016/j.jsxm.2017.08.006

Peer reviewed



Published in final edited form as:

J Sex Med. 2017 October ; 14(10): 1177–1186. doi:10.1016/j.jsxm.2017.08.006.

Altered Penile Caveolin Expression in Diabetes: Potential Role in Erectile Dysfunction

Jay Parikh, BS¹, Alice Zemljic-Harpf, MD², Johnny Fu, MS¹, Dimosthenis Giamouridis, MS³, Tung-Chin Hsieh, MD¹, Adam Kassan, PhD², Karnam S. Murthy, PhD⁴, Valmik Bhargava, PhD³, Hemal H. Patel, PhD², and M. Raj Rajasekaran, PhD¹

¹Department of Surgery, University of California–San Diego and San Diego VA Healthcare System, San Diego, CA, USA

²Department of Anesthesiology, University of California–San Diego and San Diego VA Healthcare System, San Diego, CA, USA

³Department of Internal Medicine, University of California–San Diego and San Diego VA Healthcare System, San Diego, CA, USA

⁴Virginia Commonwealth University, Richmond, VA, USA

Abstract

Background—The pathophysiology of increased severity of erectile dysfunction in men with diabetes and their poor response to oral pharmacotherapy are unclear. Defective vascular endothelium and consequent impairment in the formation and action of nitric oxide (NO) are implicated as potential mechanisms. Endothelial NO synthase, critical for NO generation, is localized to caveolae, plasma membrane lipid rafts enriched in structural proteins, and caveolins. Type 2 diabetes mellitus (T2DM)-induced changes in caveolin expression are recognized to play a role in cardiovascular dysfunction.

Corresponding Author: M. Raj Rajasekaran, PhD, San Diego VA Health Care System, 3350, La Jolla Village Drive, San Diego, CA 92161, USA. Tel: 858-552-8585, ext 7114; Fax: 858-552-7436; mrajasekaran@ucsd.edu.

Conflicts of Interest: The authors report no conflicts of interest.

STATEMENT OF AUTHORSHIP

Category 1

(a) Conception and Design

Alice Zemljic-Harpf; Karnam S. Murthy; Valmik Bhargava; Hemal H. Patel; M. Raj Rajasekaran

(b) Acquisition of Data

Jay Parikh; Alice Zemljic-Harpf; Johnny Fu; Dimosthenis Giamouridis; Adam Kassan; Karnam S. Murthy

(c) Analysis and Interpretation of Data

Alice Zemljic-Harpf; Karnam S. Murthy; Valmik Bhargava; Hemal H. Patel; M. Raj Rajasekaran

Category 2

(a) Drafting the Article

Jay Parikh; Alice Zemljic-Harpf; Johnny Fu; Tung-Chin Hsieh; Karnam S. Murthy; Valmik Bhargava; Hemal H. Patel; M. Raj Rajasekaran

(b) Revising It for Intellectual Content

Alice Zemljic-Harpf; Tung-Chin Hsieh; Valmik Bhargava; Hemal H. Patel; M. Raj Rajasekaran

Category 3

(a) Final Approval of the Completed Article

Alice Zemljic-Harpf; Valmik Bhargava; Hemal H. Patel; M. Raj Rajasekaran

Funding: None.

Aims—To evaluate DM-related changes to male erectile tissue in a mouse model that closely resembles human T2DM and study the specific role of caveolins in penile blood flow and microvascular perfusion using mice lacking caveolin (Cav)-1 or Cav-3.

Methods—We used wild-type C57BL6 (control) and Cav-1 and Cav-3 knockout (KO) male mice. T2DM was induced by streptozotocin followed by a high-fat diet for 4 months. Penile expressions of Cav-1, Cav-3, and endothelial NO synthase were determined by western blot, and phosphodiesterase type 5 activity was measured using [³H] cyclic guanosine monophosphate as a substrate. For hemodynamic studies, Cav-1 and Cav-3 KO mice were anesthetized, and penile blood flow (peak systolic velocity and end-diastolic velocity; millimeters per second) was determined using a high-frequency and high-resolution digital imaging color Doppler system. Penile tissue microcirculatory blood perfusion (arbitrary perfusion units) was measured using a novel PeriCam PSI system.

Outcomes—Penile erectile tissues were harvested for histologic studies to assess Cav-1, Cav-3, and endothelial NO synthase expression, phosphodiesterase type 5 activity, and blood flow, and perfusion measurements were assessed for hemodynamic studies before and after an intracavernosal injection of prostaglandin E₁ (50 ng).

Results—In T2DM mice, decreased Cav-1 and Cav-3 penile protein expression and increased phosphodiesterase type 5 activity were observed. Decreased response to prostaglandin E₁ in peak systolic velocity (33 ± 4 mm/s in Cav-1 KO mice vs 62 ± 5 mm/s in control mice) and perfusion (146 ± 12 AU in Cav-1 KO mice vs 256 ± 12 AU in control mice) was observed. Hemodynamic changes in Cav-3 KO mice were insignificant.

Clinical Translation—Our findings provide novel mechanistic insights into erectile dysfunction severity and poor pharmacotherapy that could have potential application to patients with T2DM.

Strengths and Limitations—Use of KO mice and novel hemodynamic techniques are the strengths. A limitation is the lack of direct evaluation of penile hemodynamics in T2DM mice.

Conclusion—Altered penile Cav-1 expression in T2DM mice and impaired penile hemodynamics in Cav-1 KO mice suggests a regulatory role for Cav-1 in DM-related erectile dysfunction.

Keywords

Caveolin-1; High-Fat Diet; Type 2 Diabetes; Erectile Dysfunction

INTRODUCTION

Erectile dysfunction (ED) is highly prevalent (35–90%) and severe in men with diabetes and affects quality of life.¹ Patients with diabetes do not respond well to phosphodiesterase type 5 (PDE5) inhibitor therapy, possibly because of defective endothelium and impaired nitric oxide (NO).²

Penile erection, a hemodynamic event, is initiated predominantly by the NO and cyclic guanosine monophosphate (cGMP) pathway.³ NO is generated in nerve endings and in corpus cavernosum (CC) endothelial cells (ECs) by NO synthase (NOS). The penis at rest is

in a flaccid state because of the contribution of sympathetic mediators to CC smooth muscle (SM) tone.⁴ During sexual stimulation, NO released from activation of neuronal NOS binds to soluble guanylate cyclase, increasing cGMP levels that lead to SM cell (SMC) relaxation and CC dilation.⁵ Subsequent hemodynamics stimulates the phosphatidylinositol-3-kinase and protein kinase B pathway, leading to activation of endothelial NOS (eNOS) and release of NO.⁶ Venous outflow occlusion is required for maintenance of high intracavernosal pressure and erection. Rigidity is achieved by emissary vein compression that is enhanced in part by ischiocavernosus muscles.⁷ Impaired penile hemodynamics that is mediated by defective vascular endothelium is recognized as a major contributor to ED in type 2 diabetes mellitus (T2DM).⁸ The mechanism of how this occurs remains unclear.

Endothelial NOS is localized to caveolae and lipid-rich plasma membrane micro-domains and is regulated by caveolins, which are resident scaffolding proteins.⁹ Caveolae and caveolins serve to concentrate receptors, G-proteins, and effector enzymes and are associated with regulating NO.⁹ Penile expression of caveolin-1 (Cav-1) has been found in endothelium and SM.^{10–12} Cav-1 knockout (KO) results in impaired penile SMC relaxation.^{10–12}

In the absence of Cav-1, there is enhanced cGMP degradation through increased PDE5 activity in colonic SM.¹³ PDE5 is localized to endothelial caveolae and modulates eNOS activity.¹⁴ Caveolin-3 (Cav-3) expression is largely restricted to striated and certain SMs. Cav-3 deficiency is correlated to skeletal muscle degeneration¹⁵ and could contribute to DM-related loss of ischiocavernosus muscle (ICM) strength.¹⁶ Decreased flow-mediated dilation in coronary arterioles of patients with DM from Cav-1 disruption and NOS uncoupling has been reported.¹⁷ The exact roles of caveolae and caveolins in the regulation of T2DM-related changes in erectile tissue remain unclear.

The aims of this study were to evaluate (i) DM-related changes to male erectile tissue in an animal model that closely resembles human T2DM and the contribution of caveolins in DM-related changes and (ii) the impact of Cav-1 or Cav-3 global deletion on penile hemodynamics.

METHODS

The San Diego Veterans Administration Hospital (San Diego, CA, USA) institutional animal care and use committee approved the study protocol, and all experiments were conducted in accordance with the Guidelines and Use of Laboratory Animals (National Institutes of Health, Bethesda, MD, USA). We used adult wild-type male C57BL/6J (control), Cav-1 KO, and Cav-3 KO mice in this study (n = 8 or 9 per group).

T2DM Mouse Model

Non-fasted 3-month-old wild-type male mice were injected intraperitoneally with a single dose of streptozotocin (STZ; 75 mg/kg in citrate buffer 0.1 mol/L, pH = 4.5) and switched immediately to a high-fat diet (60% kilocalories). Control mice received injections of citrate buffer 0.1 mol/L as the vehicle and were fed standard chow (4% calories). Three months after T2DM induction, serum glucose and glucose tolerance test (GTT) results confirmed the

metabolic disorder. For GTT, mice were fasted (11–12 hours), and fasting glucose levels were assessed from tail snips followed by intraperitoneal injection of glucose 1 g/kg in 0.9% NaCl and monitoring of blood glucose. For the insulin tolerance test (ITT), mice were injected with insulin intraperitoneally (0.4 mU/g body weight, which is equivalent to a total dose of 4–6.5 ng/mouse based on body weight), and blood glucose levels were monitored. An ultrasensitive mouse insulin enzyme-linked immunosorbent assay kit (catalog number 80-INSHU-E01.1; ALPCO Diagnostics, Salem, NH, USA) was used to determine endogenous serum insulin levels (nanograms per milliliter) using the protocol recommended by the vendor. Briefly, 25 μ L of each standard, control, and sample was transferred into their respective wells, followed by the addition of detection antibody 100 μ L. The microplate was incubated for 1 hour at room temperature on a microplate shaker. Incubation was continued with 3,3',5,5'-tetramethylbenzidine substrate 100 μ L for 15 minutes followed by stop solution. Absorbance at 450 nm was measured in a plate reader to determine insulin levels (nanograms per milliliter). Animals were maintained on the T2DM protocol for 4 months and euthanized to harvest tissue.

KO Mouse Models

Cav-1 KO animals were obtained from Jackson Laboratories (stock number 007083; Bar Harbor, ME, USA) and sampled from a colony maintained in house. Cav-3 KO mice were gifts from Drs Hagiwara and Kikuchi.¹⁸

Western Blot Analysis

Protein levels of Cav-1, Cav-3, and fibrosis markers (β -catenin, glycogen synthase kinase-3, small mothers against decapentaplegic 3, and transforming growth factor- β) and total eNOS were determined by western blot in penile tissues from control and T2DM mice (n = 4 each). Penile tissues (mid-shaft) were harvested and stored at -80°C . Samples were homogenized with lysis buffer (Tris 20 mmol/L [pH = 7.8], NaCl 137 mmol/L, KCl 2.7 mmol/L, MgCl₂ 1 mmol/L, 1% Triton X-100, 10% glycerol, ethylenediaminetetraacetic acid 1 mmol/L, dithiothreitol 1 mmol/L). Samples were centrifuged at 600g to 800g at 4°C and supernatant was collected. β -Mercaptoethanol and sample buffer were added to the samples and heated at 100°C for 10 minutes. Samples were loaded into 10% polyacrylamide precast gels and run at 140 V for 1.5 hours. Membranes were blocked in tris-buffered saline and tween (1%) containing 3% bovine serum albumin and incubated with primary antibodies overnight at 4°C. After washing, membranes were incubated for 2 hours in a secondary antibody (1:3,000). Blots were developed by an enhanced chemiluminescence method (Amersham Biosciences, Piscataway, NJ, USA). The light signal was detected by digital imaging. Image analysis for protein quantitation was done using ImageJ (National Institutes of Health). All blots were done in duplicate and quantitated using glyceraldehyde 3-phosphate dehydrogenase to normalize densitometry values.¹⁹

Immunostaining and Ultrastructural Studies

Penile tissue (n = 4) was fixed in formalin for light microscopy and immunostaining. Paraffin sections were subjected to antigen retrieval and incubated with a primary antibody (Cav-1, Cav-3, and platelet and endothelial cell adhesion molecule-1 [PECAM-1]; 1:200; Abcam, Cambridge, UK), followed by a secondary antibody and processed to localize

Cav-1, Cav-3, and PECAM-1 (also known as CD31, an endothelial cell marker). We also performed immunofluorescence studies using a specific antibody for total eNOS to evaluate the localization of this protein in control and T2DM mouse penises. For transmission electron microscopy, penile tissues (n = 2–3) from control and T2DM mice were fixed by perfusion (2.5% glutaraldehyde and 2% paraformaldehyde) and scanned (FEI Tecnai Spirit G2 BioTWIN Philips Eagle 16-megapixel camera; FEI, Hillsboro, OR, USA).²⁰ Images were analyzed (ImageJ) to determine caveolin numbers.

PDE5 Activity Measurement

Tissues from control and T2DM mice were homogenized, and PDE5 was isolated by immunoprecipitation. PDE5 immunoprecipitates were washed in a medium containing Tris 50 mmol/L (pH = 7.5), NaCl 200 mmol/L, and ethylenediaminetetraacetic acid 5 mmol/L and incubated at 30°C in a reaction mixture containing 2-[N-morpholino] ethanesulfonic acid 100 mmol/L (pH = 7.5), ethylenediaminetetraacetic acid 10 mmol/L, magnesium acetate 0.1 mol/L, bovine serum albumin 0.9 mg/mL, cGMP 20 μ mol/L, and [³H]cGMP. Samples were boiled, chilled, and incubated at 30°C in Tris (pH = 7.5) 20 mmol/L medium containing *Crotalus atrox* snake venom 10 μ g/ μ L. Samples were added to DEAE-Sephacel A-25 columns (GE Healthcare, Chicago, IL, USA), and radioactivity in the effluent was counted. PDE5 activity was expressed as counts per minute per milligram of tissue.¹³

Doppler Penile Blood Flow Studies

For hemodynamic studies, animals were anesthetized using 1.5% isoflurane. Cavernosal artery blood flow was determined using the Vevo2100 color Doppler Duplex system with a 32- to 56-MHz probe (FUJIFILM VisualSonics Inc, Toronto, ON, Canada). Blood flow was measured at baseline and after intracavernosal injection of prostaglandin E₁ (PGE₁; 50 ng). Peak systolic velocity (PSV) and end-diastolic velocity were measured.²¹

Penile Tissue Microcirculatory Perfusion

Microcirculatory blood perfusion was measured using a Peri-Cam PSI system (Perimed, Stockholm, Sweden). This system uses a non-invasive laser speckle contrast (LSC) analysis technique to quantitate (in arbitrary units) perfusion in three dimensions. Penile perfusion was measured before and after an intracavernosal injection of PGE₁ (50 ng). Data were analyzed using PIMSoft (Perimed).²²

Statistical Analysis

Data (mean \pm standard error of the mean) were analyzed using Student t-test or two-way analysis of variance using GraphPad Prism (GraphPad Software, Inc, La Jolla, CA, USA). A *P* value less than .05 was considered statistically significant.

RESULTS

T2DM Induction

Three months after T2DM induction, we detected impaired GTT reactions (Figure 1A). Insulin administration lowered increased serum glucose levels in obese and control mice

(Figure 1B). Figures 1C and 1D show the area under the curve after the GTT and ITT. Based on obesity, hyperglycemia, and insulin responsiveness, mice were considered to have T2DM. These T2DM mice showed an increased body weight compared with control mice (48 vs 31 g, respectively) and increased fasting glucose levels (233 vs 105 mg/dL; Figure 1E–G).

Immunofluorescence Studies (Cav-1, Cav-3, PECAM-1, and eNOS)

Figure 2A shows the localization of Cav-1, Cav-3, and PECAM-1 (CD31) in control and T2DM mice penises. Cav-1 immuno-labeling was observed throughout the cavernosal sinusoids. A noticeable decrease in Cav-1 and Cav-3 was observed in penises of T2DM mice. Cav-1 immunoreactivity was widespread (panel a) and more intense compared with Cav-3 (panel k). Figure 2A (panels g and q) also shows faint PECAM-1 (CD31) immuno-labeling in T2DM sections compared with controls (panels b and l). Specific localization of Cav-1 and its colocalization with PECAM, mostly around the endothelial lining of cavernosal sinusoids, were seen (white arrowheads; panels a, d, and e). Cav-3 was localized mostly to the cavernosal SM (white arrowheads; panel k). Figure 2B shows localization of eNOS in control (wild-type) and T2DM corpus cavernosum tissue, mostly around the endothelial lining of cavernosal sinusoids. A noticeable decrease in eNOS staining was observed in penises of T2DM mice (panels e, g, and h).

Ultrastructural Studies

Electron micrographic images of the CC ultrastructure show the EC lining, SMCs, subcellular collagen, and regular alignment of caveolae in the penile tissue of control and T2DM mice (Figure 3A, 3E). There was no significant difference in the number of endothelial caveolae ($4.35/\mu\text{m}$ in T2DM mice vs $4.89/\mu\text{m}$ in controls) between these animals. Control animals showed SMCs with several protrusions making cell-cell communications (Figure 3D), whereas T2DM animals lacked these protrusions (Figure 3H).

Western Blot Analysis

Decreased levels of Cav-1 and Cav-3 are shown in Figure 4A in T2DM mice (Figure 4B). A 50% decrease in Cav-1 (Figure 4B) protein was observed compared with 34% for Cav-3. Western blot and image analysis for transforming growth factor- β , small mothers against decapentaplegic 3, and β -catenin (Figure 4C) showed a significant increase in T2DM mice. T2DM mice showed an increase in PDE5 protein levels (Figure 4D). A significant decrease in eNOS also was observed in T2DM penile tissues compared with controls (Figure 4E).

PDE5 Activity

A 58% increase in PDE5 activity was observed in T2DM mice (416 ± 44 cpm/mg protein) compared with controls (264 ± 31 cpm/mg protein; Figure 4F).

Doppler Penile Blood Flow

Figures 5A to 5C show Doppler images at baseline and after PGE1 injection in control and Cav-1 and Cav-3 KO mice. PSV baseline values for control and Cav-1 and Cav-3 KO mice were 39 ± 3 , 26 ± 4 , and 34 ± 4 mm/s, respectively. After PGE1 injection, an increase in PSV was observed. After PGE1 injection, peak PSV levels for control and Cav-1 and Cav-3

KO mice were 62 ± 5 , 33 ± 4 , and 60 ± 9 mm/s, respectively (Figure 5D). A significant impairment in PGE1-induced PSV was observed in Cav-1 KO mice. Cav-3 KO mice also exhibited a decreased PSV, but this was not significant.

Penile Tissue Microcirculatory Perfusion

Figure 6A shows penile tissue perfusion in a control mouse. Figure 6B shows peak penile perfusion images after PGE1 injection. Baseline values of perfusion for control and Cav-1 and Cav-3 KO mice were 127 ± 17 , 66 ± 6 , and 48 ± 5 AU, respectively. PGE1 injection increased perfusion in all animals. Perfusion levels for control and Cav-1 and Cav-3 KO mice were 256 ± 12 , 146 ± 12 , and 185 ± 14 AU, respectively. A significant impairment in penile perfusion was observed in Cav-1 KO animals (Figure 6C). Cav-3 KO mice also exhibited decreased perfusion, but this was not significant (Figure 6C).

DISCUSSION

The aims of this study were to (i) determine whether T2DM induced by STZ and a high-fat diet would lead to penile tissue abnormalities that would affect erectile function and (ii) understand the underlying molecular mechanisms and specifically evaluate the role of caveolae and caveolins in this pathophysiology. We used a model of T2DM closely resembling the clinical features of human T2DM to evaluate morphologic, ultrastructural, and molecular changes. Our T2DM model is consistent with previous reports.^{23,24} Our T2DM mice were obese and showed increased blood glucose and serum insulin levels at 3 months after STZ and high-fat diet treatment. In contrast, type 1 diabetes mellitus (T1DM) models induced by STZ alone show low body weights and a decrease in the amount of insulin compared with controls.²⁵ These observations support our claim that our model resembles the T2DM rather than the T1DM model. Our studies using this T2DM model showed decreases in penile Cav-1, Cav-3, and eNOS levels; therefore, in the second part of our study, we used Cav-1 and Cav-3 KO mice to evaluate the hemodynamic impact of caveolin deletion.

It is well recognized that endothelial dysfunction is a major factor in DM-associated ED pathophysiology.⁸ However, the mechanisms by which this DM-related endothelial dysfunction affects penile hemodynamics and SM relaxation in ED are not understood. Advancements are hindered by (i) a paucity of clinical studies of disease-specific patient populations (types 1 and 2),²⁶ (ii) the fact that many basic science data have stemmed from T1DM models, and (iii) the current research technology to study penile hemodynamics being obsolete and invasive. Our T2DM mouse model leads to obesity and altered GTT and ITT results, which are three characteristic features of human T2DM. Endothelial dysfunction-related ED has been shown in T2DM models,²⁷⁻²⁹ manifesting increased apoptosis in cavernosal tissue. This is accompanied by decreased EC content and decreased ratio of SMC to collagen.²⁷ Our findings corroborate previous observations of increasing fibrosis markers (western blot data) and decreasing eNOS. Our ultrastructural studies show DM dysregulates cell-cell interactions between ECs and SMCs consistent with the current literature suggesting communication between these two cell types is critical for normal

vascular function. Although the mechanism of aberrant communication noticed in the penile ultrastructure of T2DM mice is unclear, it could involve caveolins.

Endothelial NOS is localized to caveolae and is regulated by caveolins. PDE5 also is localized to endothelial caveolae and thus modulates eNOS activity.¹⁴ Cav-deficient mice have been shown to have impaired SMC relaxation^{10–12} and increased PDE5 activity.¹³ Cav deficiency also has been correlated to skeletal muscle degeneration¹⁵ and could contribute to DM-related loss of ICM strength involved in penile hemodynamics. Our observation of impairment in PGE1-induced penile blood flow and perfusion suggests SM dysfunction as another potential mechanism. In addition to EC and SMC dysfunction, cavernous fibrosis has been confirmed as an important contributing factor in DM-related ED.³⁰ We focused on important markers of fibrotic pathways (ie, transforming growth factor- β , small mothers against decapentaplegic 3, Wnt signaling, β -catenin, and glycogen synthase kinase-3) that were previously implicated in STZ-induced DM.³⁰ Our findings confirm a potential role of these fibrogenic pathways in T2DM-induced penile changes. Penile tissue fibrotic changes and increased PDE activity observed in T2DM mice are other possible contributing factors to DM-related ED.

Our results showed a defective penile hemodynamic mechanism in Cav-1 KO animals. Interestingly, Cav-3 deletion had no significant impact on penile hemodynamics, although the effect was slightly blunted, which suggests that primary hemodynamic regulation is driven by ECs and SMCs. Our findings agree with observations that Cav-1 is the most important contributor to normal urogenital function.³¹ We used (i) Doppler ultrasound to determine macro-circulation and (ii) a novel LSC imaging method to assess microcirculatory perfusion. Our results indicate a significant decrease in PSV in Cav-1 KO mice, suggesting impaired CC blood flow. In addition, Cav-1 KO mice exhibited significantly impaired microcirculation. LSC imaging is a novel technique to determine tissue perfusion in mouse and this has been shown to be effective in humans to determine endothelial function.²² Previous studies have implicated microvascular dysfunction in physiologic aging and in patients with DM and cardiovascular diseases. Thus, our LSC imaging method is a viable technique to evaluate penile microvascular perfusion in small-animal models that would be considered challenging.

Certain limitations are apparent in our study. Evaluation of the splice variants of Cav-1 and analysis of caveolin-2 would help us to understand the role of each caveolin isoform in ED. However, these parameters are beyond the scope of the present study and might be worth pursuing in future investigations. Also, we focused only on hemodynamic changes, and intracavernosal pressure measurements were not done to corroborate these findings. We hope to address these in our future studies. Moreover, we measured total eNOS expression and observed changes in expression between the control and T2DM groups. We are aware there are phosphorylation sites on eNOS that could be probed but this was not done in the present study. As with the other limitations, this was beyond the scope of the present study and might be worth pursuing in future studies that aim to associate caveolin to specific states of eNOS activation.

In summary, the T2DM mouse penis exhibited (i) decreased Cav-1, Cav-3, and eNOS levels; (ii) increased fibrosis; (iii) increased PDE5 activity; and (iv) impaired penile blood flow and perfusion in Cav-1 KO mice. Our novel studies show for the first time that decreased Cav-1 and Cav-3 protein levels are found in male erectile tissue of T2DM mice. Our findings confirm a regulatory role for Cav-1 in penile hemodynamics and raise the possibility of targeting the upregulation of caveolin as a novel strategy to treat DM-related ED. However, our present study has some limitations. We recognize that evaluation of penile hemodynamics in T2DM mice would have provided direct, additional proof of concept. However, the impact of vascular risk factors such as DM on penile hemodynamics has been confirmed in humans.³² Our focus was to identify the cellular mechanism for this impairment, and the present studies provide evidence for the role of Cav-1.

Acknowledgments

The technical help of Yaozhi (Walter) Wang with histology is acknowledged.

References

1. Penson DF, Latini DM, Lubeck DP, et al. Do impotent men with diabetes have more severe erectile dysfunction and worse quality of life than the general population of impotent patients? Results from the Exploratory Comprehensive Evaluation of Erectile Dysfunction (ExCEED) database. *Diabetes Care*. 2003; 26:1093–1099. [PubMed: 12663579]
2. Condorelli RA, Calogero AE, Favilla V, et al. Arterial erectile dysfunction: different severities of endothelial apoptosis between diabetic patients “responders” and “non responders” to sildenafil. *Eur J Intern Med*. 2013; 24:234–240. [PubMed: 23357410]
3. Dean RC, Lue TF. Physiology of penile erection and pathophysiology of erectile dysfunction. *Urol Clin North Am*. 2005; 32:379–395. v. [PubMed: 16291031]
4. Andersson KE. Erectile physiological and pathophysiological pathways involved in erectile dysfunction. *J Urol*. 2003; 170:S6–S13. discussion S13–S14.
5. Burnett AL. Nitric oxide regulation of penile erection: biology and therapeutic implications. *J Androl*. 2002; 23:S20–S26. [PubMed: 12236169]
6. Hurt KJ, Musicki B, Palese MA, et al. Akt-dependent phosphorylation of endothelial nitric-oxide synthase mediates penile erection. *Proc Natl Acad Sci U S A*. 2002; 99:4061–4066. [PubMed: 11904450]
7. Hsu GL, Hsieh CH, Wen HS, et al. Anatomy of the human penis: the relationship of the architecture between skeletal and smooth muscles. *J Androl*. 2004; 25:426–431. [PubMed: 15064322]
8. Castela A, Costa C. Molecular mechanisms associated with diabetic endothelial-erectile dysfunction. *Nat Rev Urol*. 2016; 13:266–274. [PubMed: 26878803]
9. Patel HH, Murray F, Insel PA. Caveolae as organizers of pharmacologically relevant signal transduction molecules. *Annu Rev Pharmacol Toxicol*. 2008; 48:359–391. [PubMed: 17914930]
10. Shakirova Y, Hedlund P, Sward K. Impaired nerve-mediated relaxation of penile tissue from caveolin-1 deficient mice. *Eur J Pharmacol*. 2009; 602:399–405. [PubMed: 19068211]
11. Linder AE, Leite R, Lauria K, et al. Penile erection requires association of soluble guanylyl cyclase with endothelial caveolin-1 in rat corpus cavernosum. *Am J Physiol Regul Integr Comp Physiol*. 2006; 290:R1302–R1308. [PubMed: 16373436]
12. Bakircioglu ME, Sievert KD, Nunes L, et al. Decreased trabecular smooth muscle and caveolin-1 expression in the penile tissue of aged rats. *J Urol*. 2001; 166:734–738. [PubMed: 11458126]
13. Mahavadi S, Bhattacharya S, Kumar DP, et al. Increased PDE5 activity and decreased Rho kinase and PKC activities in colonic muscle from caveolin-1^{-/-} mice impair the peristaltic reflex and propulsion. *Am J Physiol Gastrointest Liver Physiol*. 2013; 305:G964–G974. [PubMed: 24157969]

14. Gebska MA, Stevenson BK, Hemnes AR, et al. Phosphodiesterase-5A (PDE5A) is localized to the endothelial caveolae and modulates NOS3 activity. *Cardiovasc Res.* 2011; 90:353–363. [PubMed: 21421555]
15. Ohsawa Y, Hagiwara H, Nakatani M, et al. Muscular atrophy of caveolin-3-deficient mice is rescued by myostatin inhibition. *J Clin Invest.* 2006; 116:2924–2934. [PubMed: 17039257]
16. Murray FT, Johnson RD, Sciadini M, et al. Erectile and copulatory dysfunction in chronically diabetic BB/WOR rats. *Am J Physiol Endocrinol Metab.* 1992; 263:E151–E157.
17. Cassuto J, Dou H, Czikora I, et al. Peroxynitrite disrupts endothelial caveolae leading to eNOS uncoupling and diminished flow-mediated dilation in coronary arterioles of diabetic patients. *Diabetes.* 2014; 63:1381–1393. [PubMed: 24353182]
18. Hagiwara Y, Sasaoka T, Araishi K, et al. Caveolin-3 deficiency causes muscle degeneration in mice. *Hum Mol Genet.* 2000; 9:3047–3054. [PubMed: 11115849]
19. Wilkes N, White S, Stein P, et al. Phosphodiesterase-5 inhibition synergizes rho-kinase antagonism and enhances erectile response in male hypertensive rats. *Int J Impot Res.* 2004; 16:187–194. [PubMed: 15073608]
20. Wang J, Schilling JM, Niesman IR, et al. Cardioprotective trafficking of caveolin to mitochondria is Gi-protein dependent. *Anesthesiology.* 2014; 121:538–548. [PubMed: 24821070]
21. Sikka SC, Hellstrom WJ, Brock G, et al. Standardization of vascular assessment of erectile dysfunction: standard operating procedures for duplex ultrasound. *J Sex Med.* 2013; 10:120–129.
22. Verri V, Brandao A, Tibirica E. The evaluation of penile microvascular endothelial function using laser speckle contrast imaging in healthy volunteers. *Microvasc Res.* 2015; 99:96–101. [PubMed: 25843506]
23. Skovso S. Modeling type 2 diabetes in rats using high fat diet and streptozotocin. *J Diabetes Investig.* 2014; 5:349–358.
24. Fricovsky ES, Suarez J, Ihm SH, et al. Excess protein O-GlcNAcylation and the progression of diabetic cardiomyopathy. *Am J Physiol Regul Integr Comp Physiol.* 2012; 303:R689–R699. [PubMed: 22874425]
25. Furman BL. Streptozotocin-induced diabetic models in mice and rats. *Curr Protoc Pharmacol.* 2015; 70:5.47.1–5.47.20.
26. Chitale K. Type 1 and type 2 diabetic-erectile dysfunction: same diagnosis (ICD-9), different disease? *J Sex Med.* 2009; 6(Suppl 3):262–268. [PubMed: 19267848]
27. Xie D, Odronic SI, Wu F, et al. Mouse model of erectile dysfunction due to diet-induced diabetes mellitus. *Urology.* 2007; 70:196–201. [PubMed: 17656247]
28. Luttrell IP, Swee M, Starcher B, et al. Erectile dysfunction in the type II diabetic db/db mouse: impaired venoocclusion with altered cavernosal vasoreactivity and matrix. *Am J Physiol Heart Circ Physiol.* 2008; 294:H2204–H2211. [PubMed: 18326798]
29. Wingard C, Fulton D, Husain S. Altered penile vascular reactivity and erection in the Zucker obese-diabetic rat. *J Sex Med.* 2007; 4:348–362. discussion 362–363. [PubMed: 17367430]
30. Shin SH, Kim WJ, Choi MJ, et al. Aberrant expression of Wnt family contributes to the pathogenesis of diabetes-induced erectile dysfunction. *Andrology.* 2014; 2:107–116. [PubMed: 24265248]
31. Woodman SE, Cheung MW, Tarr M, et al. Urogenital alterations in aged male caveolin-1 knockout mice. *J Urol.* 2004; 171:950–957. [PubMed: 14713860]
32. Kendirci M, Trost L, Sikka SC, et al. The effect of vascular risk factors on penile vascular status in men with erectile dysfunction. *J Urol.* 2007; 178:2516–2520. discussion 2520. [PubMed: 17937942]

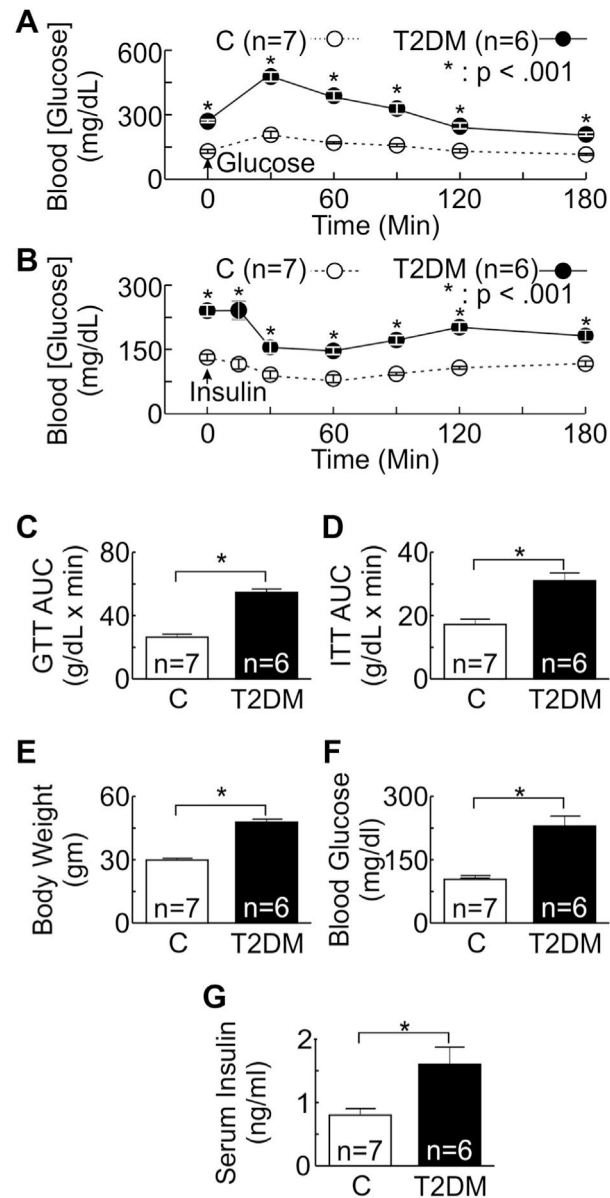
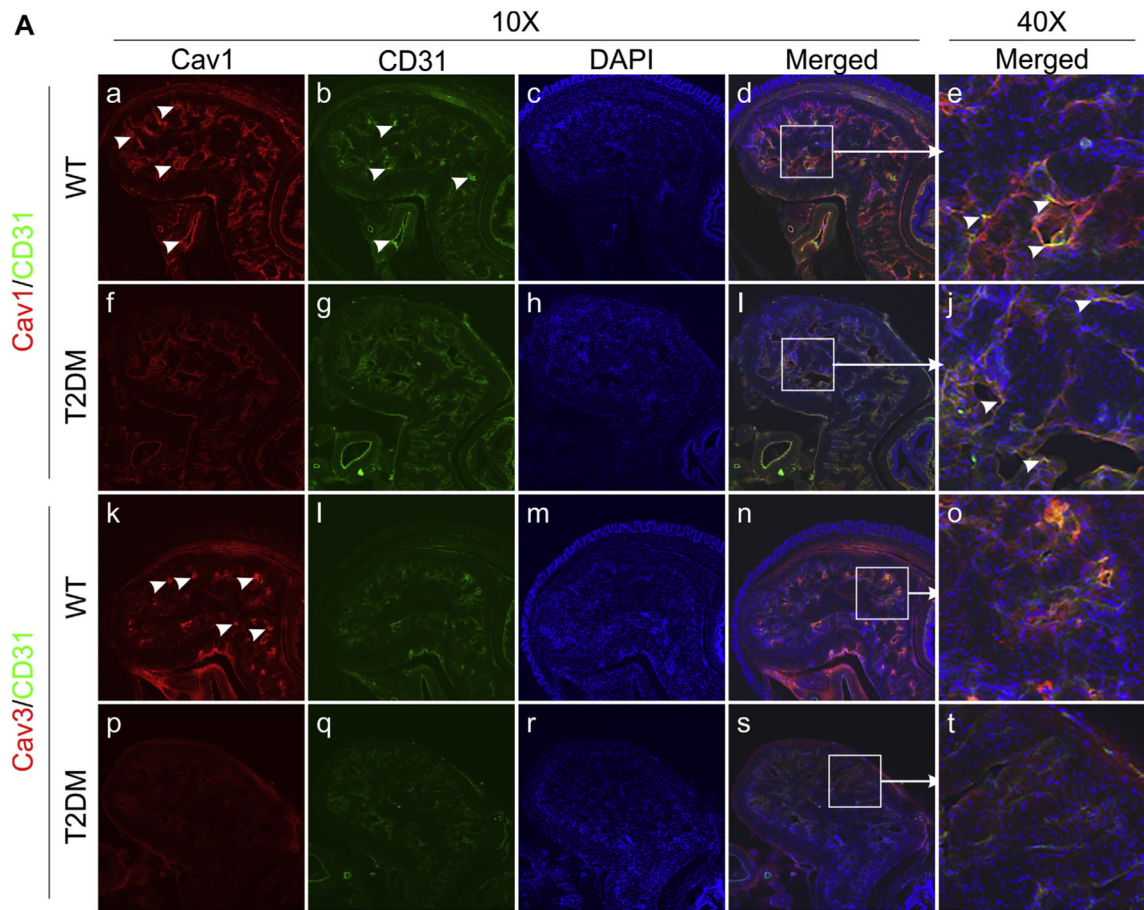


Figure 1.

Comparison of GTT and ITT in T2DM and control mice. Panel A shows impaired glucose tolerance compared with control littermates on normal chow. Panel B shows that insulin administration lowered increased serum glucose levels in obese and control mice. Panel C shows a significant increase in the area under the curve for T2DM after GTT. Panel D shows a significant increase in the area under the curve after ITT. Panel E shows body weight changes. Panel F shows fasting blood glucose levels 3 months after T2DM induction. Panel G shows serum insulin levels 3 months after T2DM induction. * $P < .05$. C = control; GTT = glucose tolerance test; ITT = insulin tolerance test; T2DM = type 2 diabetes mellitus.



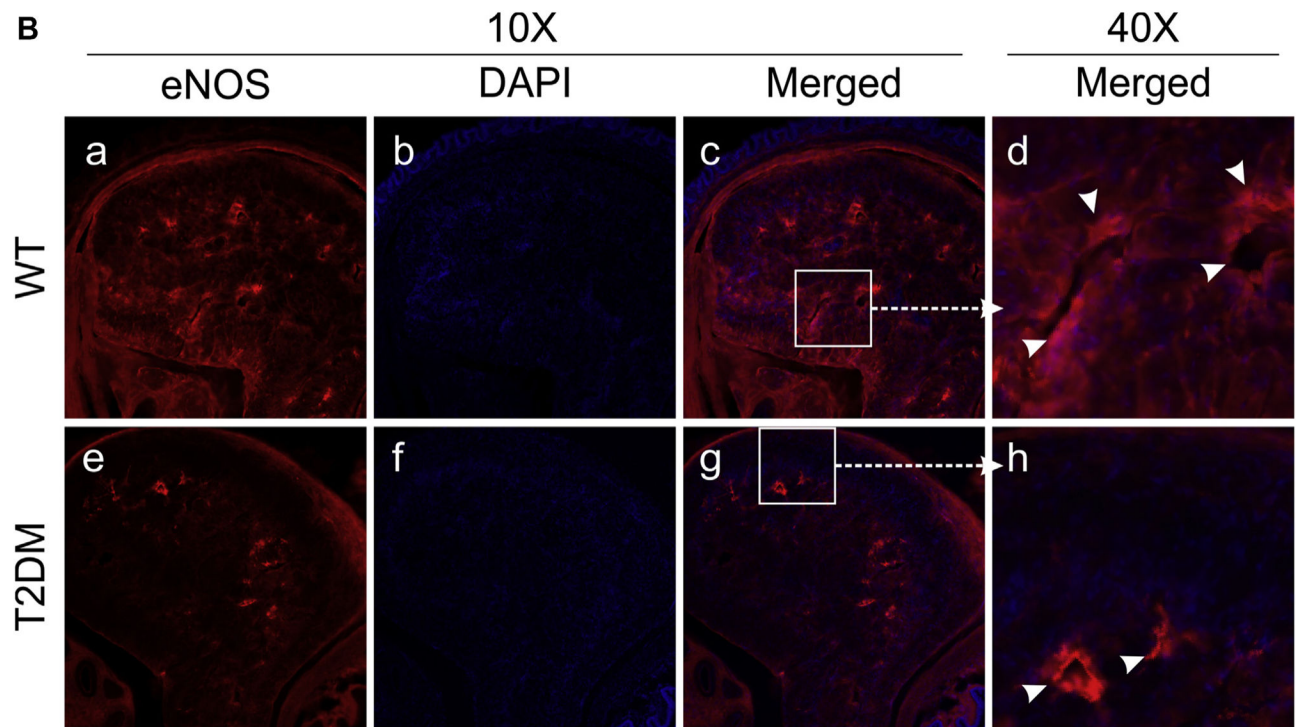


Figure 2.

Panel A shows fluorescence images of immuno-labeling for Cav1 and Cav3 (red areas in panels a, f, k, p) and an endothelial marker, platelet and endothelial cell adhesion molecule-1 (CD31; green areas in panels b, g, l, q), in penile tissue cross-sections from control (WT) and T2DM mice. Specific localization of Cav1 and its colocalization with platelet and endothelial cell adhesion molecule-1, mostly around the endothelial lining of cavernosal sinusoids, are seen (white arrowheads in panels a, d, e). Cav3 is localized to the cavernosal smooth muscle (white arrowheads in panel k). The yellow area on the merged images denotes a doubly positive area for Cav1 and platelet and endothelial cell adhesion molecule-1. Inset shows magnified image. Note decreased Cav1 and Cav3 staining in T2DM mouse corpus cavernosum tissue. Magnifications = 10 \times and 40 \times . Panel B shows fluorescence images of immuno-labeling for eNOS in penile tissue cross-sections from control (WT; panels a, c, d) and T2DM (panels e, g, h) mice. Specific localization of eNOS around the endothelial lining is shown with white arrowheads. Note the decreased eNOS staining in T2DM mouse corpus cavernosum tissue. Inset shows magnified image. Magnifications = 10 \times and 40 \times . Cav1 = caveolin-1; Cav3 = caveolin-3; DAPI = 4',6-diamidino-2-phenylindole; sNOS = endothelial nitric oxide; T2DM = type 2 diabetes mellitus; WT = wild type. Figure 2 is available online at www.jsm.jsexmed.org.

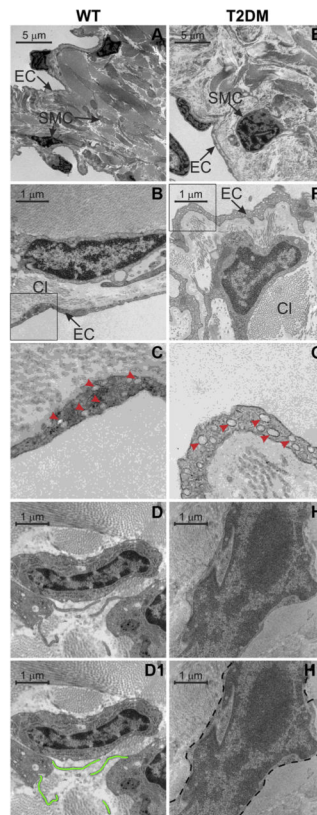
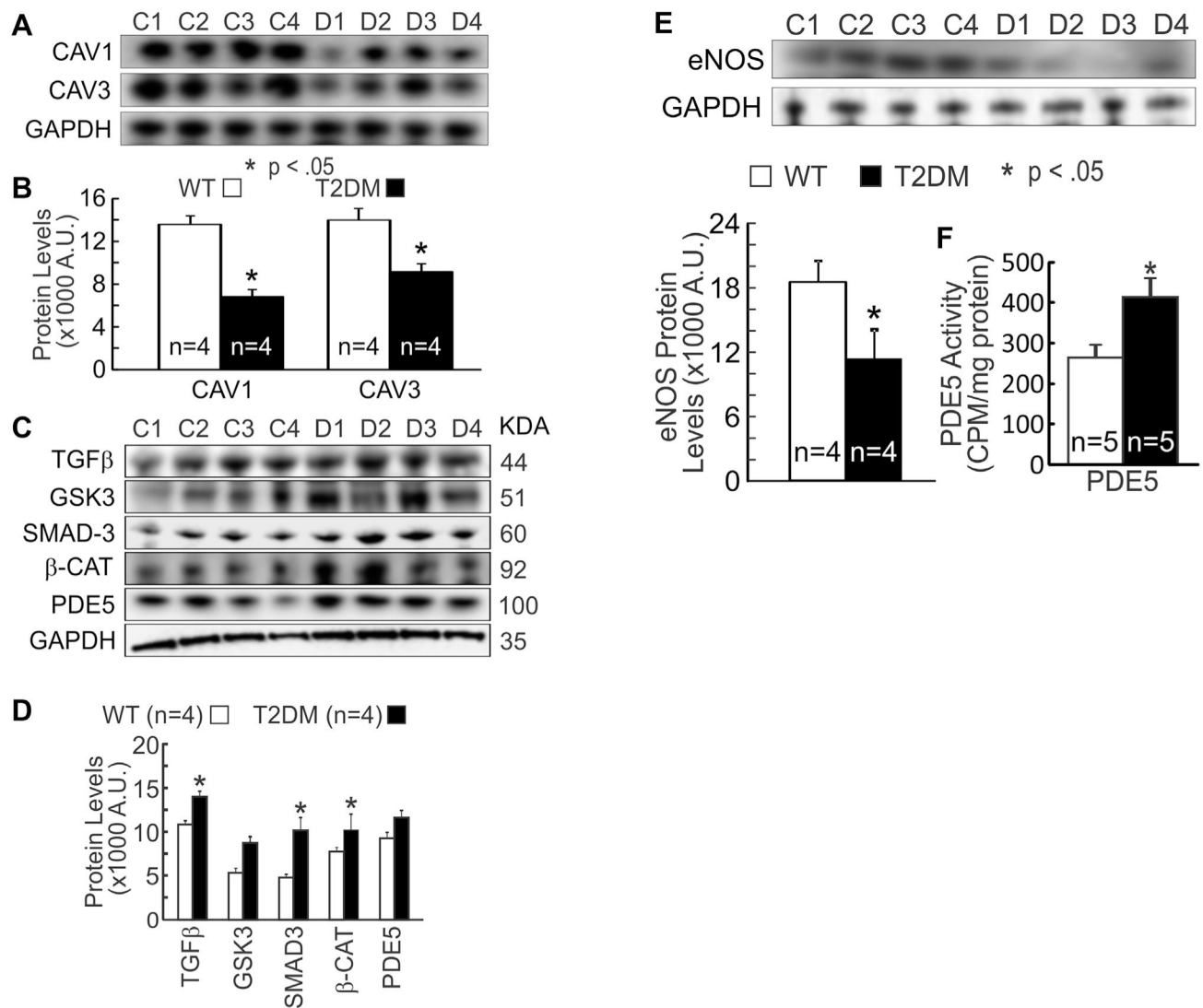


Figure 3. Representative electron microscopic images showing the corpus cavernosum ultrastructure from control (WT; left panel) and T2DM (right panel) mice. Panels A and E show the ultrastructural organization of important organelles such as the endothelial cell lining and smooth muscle cells. Panels B and F show caveolins on the endothelial cell lining and intracellular collagen. Panels C and G show zoomed regions of the insets from panels B and F displaying endothelial cell lining caveolins (red arrows). Panel D shows active smooth muscle cells with a nucleus and several protrusions making cell-to-cell communications. These protrusions are identified by green lines (D1). Panel H shows the nucleus and the smooth muscle cell without any protrusions. The area for comparison is marked by a black dotted line (H1). Cav1 = caveolin-1; Cav3 = caveolin-3; T2DM = type 2 diabetes mellitus; WT = wild type. Figure 3 is available online at www.jsm.jssexmed.org.

**Figure 4.**

Panel A shows western blot gel for Cav1 and Cav3 in control (C1–C4) and T2DM (D1–D4) mice. GAPDH was used to normalize Cav1 and Cav3 values. Panel B shows a significant decrease in Cav1 and Cav3 in T2DM mice compared with control (WT) mice. Panel C shows western blot gels for fibrosis markers. Panel D shows a significant increase in TGFβ, SMAD-3, β-CAT, and protein penile levels in T2DM mice (D1–D4) compared with control mice (C1–C4). Protein levels of GSK3 and PDE5 showed an increase in T2DM but the increase was not significant. Panel E (top) shows western blot gel for eNOS in control (C1–C4) and T2DM (D1–D4) mice. GAPDH was used to normalize Cav1 and Cav3 values. Panel E (bottom) bar graph shows a significant decrease in eNOS in T2DM compared with control mice. Panel F shows biochemical analysis indicating a significant increase in PDE5 activity in T2DM compared with control mice. * $P < .05$. β-CAT = β-catenin; Cav1 = caveolin-1; Cav3 = caveolin-3; eNOS = endothelial nitric oxide; GAPDH = glyceraldehyde 3-phosphate dehydrogenase; GSK3 = glycogen synthase kinase-3; PDE5 = phosphodiesterase type 5;

SMAD3 = small mothers against decapentaplegic 3; T2DM = type 2 diabetes mellitus; TGF- β = transforming growth factor- β ; WT = wild type.

Author Manuscript

Author Manuscript

Author Manuscript

Author Manuscript

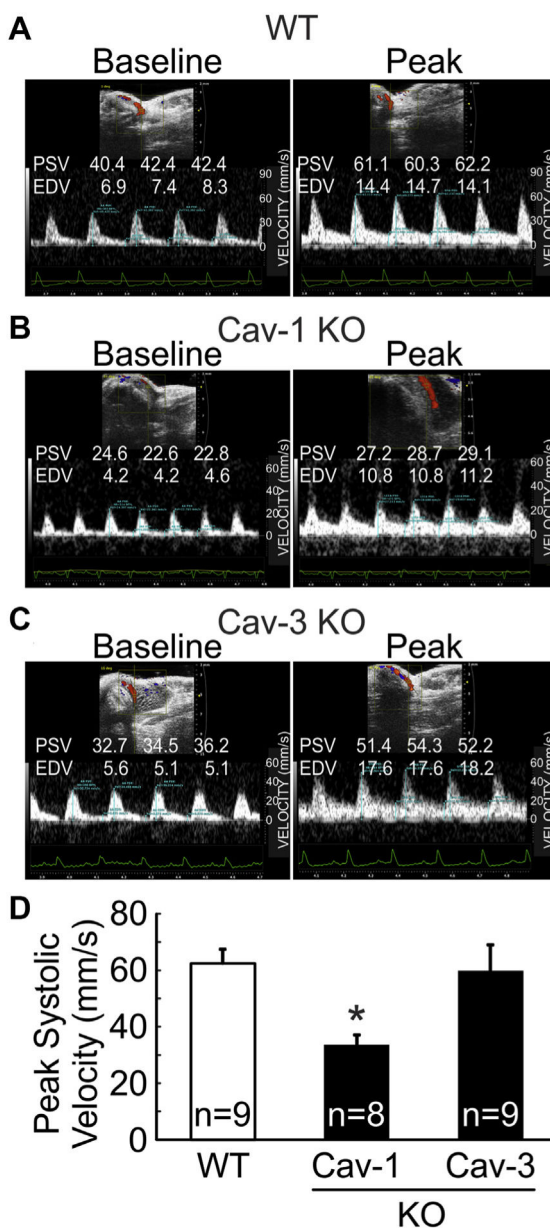


Figure 5. Panels A, B, and C show Doppler flow velocity from control (WT), Cav-1 KO, and Cav-3 KO mice, respectively, at baseline and after prostaglandin E₁ injection. Panel D shows bar graph of mean values of PSV in control (WT), Cav-1 KO, and Cav-3 KO mice. Cav-1 KO mice showed a significant decrease in PSV, whereas Cav-3 KO animals did not. * $P < .05$. Cav-1 = caveolin-1; Cav-3 = caveolin-3; EDV = end-diastolic velocity; KO = knockout; PSV = peak systolic velocity; WT = wild type. Figure 5 is available online at www.jsm.jssexmed.org.

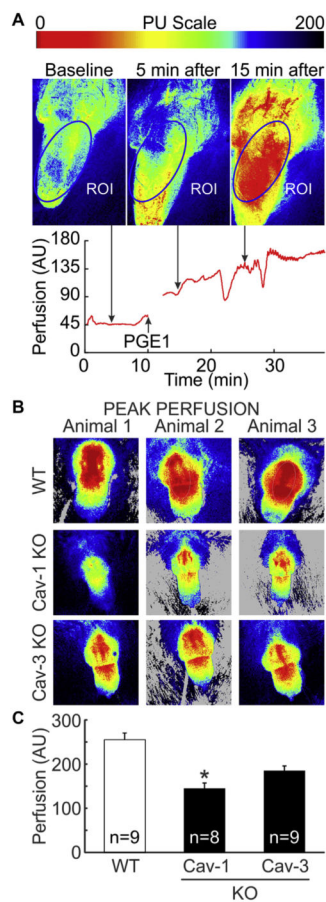


Figure 6.

Panel A shows representative images of the time course of PGE1 injection-induced changes to penile blood perfusion in control mice (WT). Panel B shows three representative peak perfusion images from control (WT), Cav-1 KO, and Cav-3 KO mice. Panel C shows a bar graph of mean values of peak penile perfusion in control (WT), Cav-1 KO, and Cav-3 mice. Cav-1 KO mice had a significant decrease in penile blood perfusion, whereas the decrease in Cav-3 KO animals was not significant. $*P < .05$. Cav-1 = caveolin-1; Cav-3 = caveolin-3; KO = knockout; PGE1 = prostaglandin E₁; ROI = region of interest; WT = wild type. Figure 6 is available online at www.jsm.jsexmed.org.